THE JOURNAL OF PHYSICAL CHEMISTRY B

Article

pubs.acs.org/JPCB

Infrared, Vibrational Circular Dichroism, and Raman Spectral Simulations for β-Sheet Structures with Various Isotopic Labels, Interstrand, and Stacking Arrangements Using Density Functional Theory

William R. W. Welch,[†] Jan Kubelka,*[,†] and Timothy A. Keiderling*[,‡]

[†]Department of Chemistry, University of Wyoming, Laramie, Wyoming 82071, United States

[‡]Department of Chemistry, University of Illinois at Chicago, 845 West Taylor Street (m/c 111), Chicago Illinois 60607, United States

Supporting Information

ABSTRACT: Infrared (IR), Raman, and vibrational circular dichroism (VCD) spectral variations for different β-sheet structures were studied using simulations based on density functional theory (DFT) force field and intensity computations. The DFT vibrational parameters were obtained for β-sheet fragments containing nine-amides and constrained to a variety of conformations and strand arrangements. These were subsequently transferred onto corresponding larger β-sheet models, normally consisting of five strands with ten amides each, for spectral simulations. Further extension to fibril models composed of multiple stacked β-sheets was achieved by combining the transfer of DFT parameters for each sheet with dipole coupling methods for interactions between sheets. IR spectra of the amide I show different splitting patterns for parallel and antiparallel β-sheets, and their VCD, in the absence of intersheet stacking, have distinct sign variations. Isotopic labeling by ^{13}C of selected residues yields spectral shifts and intensity changes uniquely sensitive to relative alignment of strands (registry) for antiparallel sheets. Stacking of multiple planar sheets maintains the qualitative spectral character of the single sheet but evidences some reduction in the exciton splitting of the amide I mode. Rotating sheets with respect to each other leads to a significant VCD enhancement, whose sign pattern and intensity is dependent on the handedness and degree of rotation. For twisted β-sheets, a significant VCD enhancement is computed even for sheets stacked with either the same or opposite alignments and the intersheet rotation, depending on the sense, can either further increase or weaken the enhanced VCD intensity. In twisted, stacked structures (without rotation), similar VCD amide I patterns (positive couplets) are predicted for both parallel and antiparallel sheets, but different IR intensity distributions still enable their differentiation. Our simulation results prove useful for interpreting experimental vibrational spectra in terms of β-sheet and fibril structure, as illustrated in the accompanying paper.

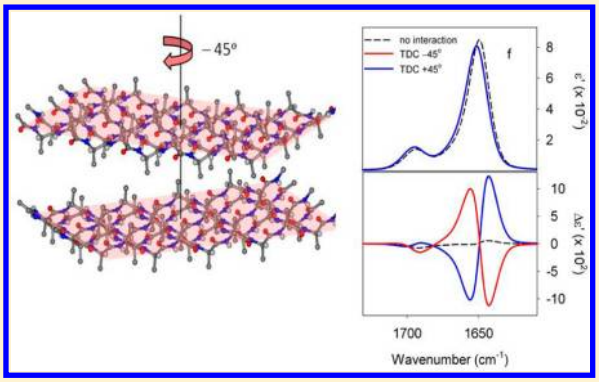

INTRODUCTION

Characterization of secondary structural content in peptides and proteins has long been an important application of infrared (IR) spectroscopy,[1−3] which is often used in conjunction with other optical spectroscopic methods, such as circular dichroism (CD).[4] While CD is very useful for α-helix determination, IR is a particularly strong method for evaluation of β-sheet structure, making these approaches complementary. However, β-sheets are essentially tertiary structures stabilized by interactions between two or more strands (which are effectively independent, i.e., not required to be adjacent in the sequence) via H-bonding to form a sheet. These sheets exist in a variety of interstrand arrangements, most notably as parallel or antiparallel. In addition, the strands can be in- or out-of-register, meaning that all the hydrogen bonds on the neighboring strands are satisfied or that some (terminal residues) are left unpaired, respectively. Further, the sheet may be essentially flat, or its plane may twist to form a variety of three-dimensional structures including stacking of multiple sheets into aggregate and fibril forms.[5] Recent interest in such self-assembled structures is driven in a large part by their role as a common structural aspect of proteins and peptides associated with neurodegenerative symptoms in such conditions as Alzheimer's, Parkinson's, and many other diseases.[6] The individual sheets within these stacks can also be aligned with the same or opposite sense or with a relative angular rotation caused by or contributing to the fibril helicity.[7,8] Differentiation of these various structural types using a rapid spectroscopic probe is naturally an important goal.

IR studies of the amide I band have generally provided an important tool for such conformational discrimination, since the antiparallel β-sheet yields an exciton split spectrum with a

Received: June 6, 2013
Revised: August 2, 2013

   dx.doi.org/10.1021/jp4056126 | J. Phys. Chem. B XXXX, XXX, XXX−XXX

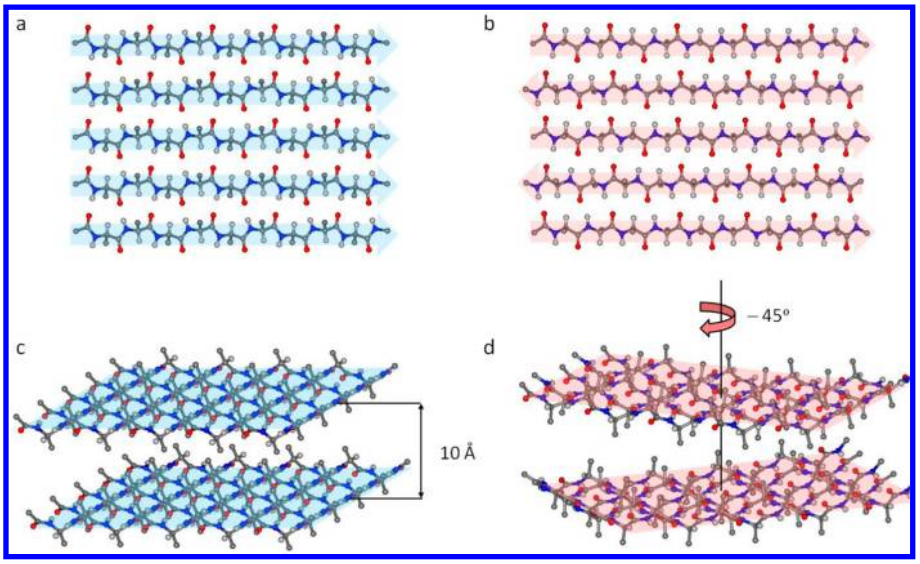

Figure 1. Examples of model β-sheet structures used for spectra simulations: (a) five-stranded parallel β-sheet (φ = −138°, ψ = 134°), (b) five-stranded antiparallel β-sheet (φ = −119°, ψ = 113°), (c) two stacked parallel β-sheets, separated by 10 Å, 0° orientation, and (d) two stacked antiparallel β-sheets, separated by 10 Å, in −45° orientation.

dominant low frequency mode (1620−1630 cm^{-1}) and a weaker but clearly detectable high frequency component (1680−1690 cm^{-1}).[9−13] By contrast, the parallel sheet has been predicted to lack the high frequency band and often its lower frequency, intense component occurs at higher wavenumbers.[9−11,14,15] Historically, this pattern has been somewhat difficult to verify experimentally, since most model peptides form antiparallel aggregates while parallel structures were normally restricted to protein structures where they were limited in length and usually twisted. However, some protein fibril structures have been determined to have local parallel strand structures, while antiparallel fibrils have been found for shorter oligomers, making the array of potential conformers now more complex.[7,8] In addition, fibrils have intersheet interactions which add a new dimension to interpreting spectral patterns.[16] More recently it has been suggested that vibrational circular dichroism (VCD)[9,17,18] and polarized Raman[17] as well as nonlinear[19] and 2D IR[20−23] can also be used to discriminate sheet types.

In an alternate approach, various IR studies have used isotopic labels, mostly ^{13}C on the amide C═O to cause a shift of that component of the amide I down by ∼40 cm^{-1}, and consequently provide site-specific sensitivity for vibrational spectroscopic studies of peptide structures.[22,24−28] These studies effectively follow the logic of successful NMR experiments that use dipole coupling of isotopically labeled residues to determine distances and measures of fibril geometries.[8,29−31] It was assumed that interstrand coupling, which is highly distance dependent, would lead to unique shifts of the labeled band to allow discrimination of sheet types by labeling them in different positions.[26,32−36] For example, parallel sheets with the same single label in each strand would have identical coupling between labels for all positions, while antiparallel sheets in register would have maximum coupling for labels in the center of a strand, as compared to those closer to the termini, which are spatially far apart. Of course, for strands out of register this would be more complex. While such a design assumption may seem obvious, it has not been tested in detail from a higher level, theoretical point of view, which we address in this paper.

Most β-sheet labeling studies were done on independent β-strands that interact to form extended sheets and possibly aggregates.[26,32−39] More controlled experiments utilized β-hairpins, which have less regular sheet structure but are monomeric and have antiparallel alignment with constrained strand registry.[19,20,40−47] These show cross strand coupling effects, but the expected frequency shifts were not so evident. In fact, unique coupling patterns with oppositely signed coupling constants were found to be dependent on the interstrand H-bonding pattern between the two labeled C═O groups. Such complications could also arise in multistrand structures depending on whether the strands were in or out of register.[26,29,33,34]

While analysis of these IR isotope effects was initially done based on empirical correlations, several theoretically based interpretive schemes have subsequently been proposed. Most have been based on some variant of transition dipole coupling (TDC) empirically parametrized to improve agreement with experiment.[13,15−18,38] However, it has long been recognized[48] that TDC is insufficient for modeling vibrational coupling of the neighboring amides. For this reason, more recent simulations include local coupling constants derived from maps based on higher order models such as dipeptide *ab initio* (or density functional theory, DFT) computations.[20−22,32] Our approach has been fundamentally different in that we have used vibrational parameters (Cartesian force field, FF, and atomic polar tensors, APT) derived from DFT calculations.[49] These are subsequently transferred onto larger model molecules via a Cartesian coordinate transfer (CCT),[50] carried out directly without any additional approximations, such as transformation to local modes and coupling of them based on small peptide fragment calculations.[11,12,51] Over the past decade, we have extensively tested this methodology as well as additional possible improvements on a variety of systems, including β-sheet structures.[49,52] In particular, we proposed the basic distinctions expected for parallel and antiparallel β-sheets, the effects of twist and number of strands,[9,53] as well as ^{13}C isotopic effects.[39,54] Many of these observations were subsequently reproduced in simpler calculations when sufficient interactions were included.[11,16,17,32]

dx.doi.org/10.1021/jp4056126 | J. Phys. Chem. B XXXX, XXX, XXX−XXX

The DFT calculations combined with the CCT methodology also allowed us to directly test TDC.[55] Specifically in β-sheets we found TDC to be generally a poor approximation for intrastrand vibrational couplings. For the interstrand coupling, the TDC performed better but still failed to reproduce the DFT spectra. While simplified calculations may have practical value, it is important to confirm that they adequately represent the underlying interactions. Thus, developing a systematic comparison to higher level calculations is important.

In addition to IR, DFT calculations can also be used to compute vibrational circular dichroism (VCD) as well as Raman and Raman optical activity (ROA) spectra, by adding atomic axial (magnetic dipole, AAT) and polarizability tensors, and can be extended to include solvent effects.[49,56−61] Furthermore, DFT based calculations naturally yield spectra for all harmonic modes of the computed structure, allowing spectral predictions for a variety of amide-centered vibrations, since they are not limited to a model oscillator correlated to the amide I local mode. Finally, these methods can also be used to optimize structures, should that be a goal.

In this paper, we report simulations of IR, VCD, and Raman spectra for several model β-sheet structures that are most relevant to the problems of aggregation and fibril formation, including multisheet, stacked structures. In particular, we focus on potential applications of ^{13}C isotope labeling, as the ^{13}C═O amide I bands can provide a definitive marker of the strand arrangement. Our goal is to provide a general overview of the potential capabilities of vibrational spectroscopic methods in studying the structure of β-sheet aggregates and fibrils from a nonempirical theoretical perspective. In an accompanying paper,[62] we provide specific examples of how our calculations can be used to interpret previously published experimental data in terms of the β-sheet structural parameters.

METHODS

Model Structures. The β-sheet models were constructed as capped oligo-alanine strands, typically Ac-Ala$_9$-NH−CH$_3$, assembled into five-stranded sheets (Figure 1). The sheet geometries were obtained using standard antiparallel (φ = −138°, ψ = 134°) and parallel (φ = −119°, ψ = 113°) β-sheet structures, as reported previously.[9] (We note that in ref 9 the φ angles were erroneously listed as positive.) Increasing the number of strands beyond five appeared to have only a minor effect on the spectra (Figure S1, Supporting Information, SI). Smaller sheets either with shorter strands (five strands of five amides each) or with fewer strands (three strands of ten amides each) were used for investigation of the effects of stacking interactions, for which stacks of up to five β-sheets were considered. In addition, the influence of the β-sheet twist was tested using model sheet geometries derived from protein structures, as detailed before.[9] In both these model parallel and antiparallel structures, the strands have a left-handed helical twist of approximately −5° per residue. For the purpose of vibrational parameter transfer and spectra simulations (see below), the hydrogen groups on the Ala and capping methyl groups (which are explicitly included in the DFT computation) were deleted in the large model structures. This not only significantly reduces the number of atoms and therefore the size of force field (FF) matrices to be diagonalized, but also eliminates vibrational interference with the fixed side-chain (methyl) groups.[52,63,64]

Density Functional Theory Calculations. DFT based atomic force field (FF) and polar (APT), axial (AAT) and polarizability tensor components were obtained by computations at the BPW91/6-31G** level using Gaussian-03 or Gaussian-09.[65] The DFT calculations were carried out for various conformations of three-stranded β-sheet fragments based on Ac-Ala$_2$-NH-CH$_3$ strands that were constrained to the same geometries as used to construct the larger sheets. Other functionals, namely, the B3LYP as well as larger basis sets (6-31++G**) were tested, as was the inclusion of the solvent (water) through an implicit, conductor-like polarized continuum model (CPCM). However, while minor differences were noted, consistent with our previous work on a variety of peptide models, the BPW91/6-31G** level is found to provide an ideal price/performance ratio for amide mode simulations. This level maintains the amide I intensity distribution over the exciton band but has a consistent shift to higher frequency from experimental values, which is mostly due to not incorporating solvation effects (see the Supporting Information, Figure S2, for a comparison).

Transfer of the Vibrational Parameters. The vibrational FF and the corresponding APT, AAT, and polarizability derivative tensors for simulating the spectra of the sheet structures were transferred from the smaller oligomer calculations to the larger sheets using routines kindly provided by Petr Bouř, Academy of Science, Prague.[50]

Simulation of Stacking Interactions. Effects of intersheet interactions were simulated by stacking two to five sheets in a superstructure and using TDC to approximate the through-space, intersheet FF parameters. Unlike empirical TDC approaches, our approximation is based on the APT obtained quantum mechanically at the DFT level,[52,55,64] and the coupling constants are incorporated into the all-atom FF. As a consequence, the TDC approximation is not limited to the amide I but contributes to all modes. Since APT are atomic parameters, the origins of the individual transition dipole components are most naturally chosen to be on their corresponding atoms. While other possibilities were tested, the resulting computed spectra are essentially independent of the details of the transition dipole positions.[52,64]

Since the TDC was previously found unsatisfactory in comparison with the DFT vibrational calculations for short-range interactions,[55] its performance for the simulations of stacked sheet spectra was tested against full DFT calculations on two sheets with two and three Ac-Ala$_2$-NH-CH$_3$ strands. The tests consisted of varying the distance as well as the orientation of the stacked sheets.

The model structures containing two stacked β-sheets were constructed from the sheets described above with five strands of ten amides each. To test the effect of multiple stacked sheets, models with three, four, and five sheets were built, but these were limited to five amides per strand (and five stranded) as the resultant calculations with five stacked sheets (125 amide groups, 1300 atoms) become quite large and do impose some limits on our computational resources. In addition, for twisted sheets where the strand length was found important, three-stranded sheets with ten amides per strand were constructed and simulations carried out for up to four stacked sheets. Larger simulations would require using alternative methods of matrix diagonalization, such as the arbitrary time-propagation method.[66]

Simulation of the Vibrational Spectra. Full FF matrices obtained with the above methods were diagonalized and the spectral intensities were computed from the dipole (APT, AAT) and polarizability derivatives using in-house codes. These

dx.doi.org/10.1021/jp4056126 | J. Phys. Chem. B XXXX, XXX, XXX−XXX

programs also allow for straightforward inclusion of isotopic substitution by simply changing the atomic masses, to simulate the effects of the isotopic editing with ^{13}C on the amide C═O. Isotopic substitution was also used to account for effects of amide deuteration, since IR and VCD spectra are typically measured for N-deuterated samples in D_2O. In addition, the Ala methyl and blocking groups, where present, were all completely deuterated to eliminate their interference in the amide II/II′ region, as done previously.[52,55,63,64] The spectral bandshapes were simulated by assigning pseudo-Voigt profiles (40% Lorentzian, 60% Gaussian), with a uniform width (fwhm) of 14 cm^{-1} and an area proportional to the total intensity, to each computed transition.

RESULTS

As is commonly a problem with studies of β-sheets, the number of variations in terms of structure and computational level possible makes the quantity of simulated spectra grow to a level that is not possible to utilize or comprehend in a meaningful manner within the constraints of a normal publication. Thus, here we present selected examples targeted at questions one might pose in studying β-sheet structures, with additional results provided in the Supporting Information. Since there are a very large number of calculations, to help guide the reader we provide a listing of the figures and their contents in the Supporting Information (Table S1).

Parallel and Antiparallel Strands. The most fundamental structural issue to address for β-sheets is the differentiation between parallel and antiparallel strands. Our calculations for both idealized flat (Figure 2) and twisted (see below) sheets with in-register strands support the generally accepted qualitative pattern[9−11,14,15] that the antiparallel IR amide I has a detectable high frequency band while the parallel does not (see Figure 2 and Figure S3 in the Supporting Information). Both structures have approximately the same amide I mode dispersion (as shown in detail in the example of Figure S3 in the Supporting Information), but the different intensity distributions among the component modes make the antiparallel amide I appear to have greater splitting (Figure 2b) than the parallel one (Figure 2a). Quantitatively, the "exciton splitting" is somewhat sensitive to the details of geometry, i.e., the degree of twist of the β-sheet plane (see below) as well as the extent (size) of sheets formed. In particular, as shown in Figure S1 in the Supporting Information, although quantitatively a small effect, increasing the number of strands in the β-sheet tends to shift the main amide I maximum lower and therefore increases the apparent splitting.

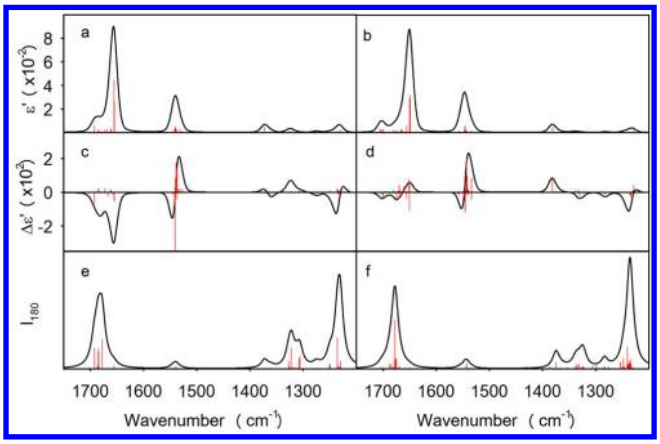

Figure 2. Vibrational spectra for idealized model β-sheets. IR (a and b), VCD (c and d), and Raman (e and f) spectra calculated for parallel (left) and antiparallel (right) sheets of five strands each having ten amides and aligned in register. The spectra were obtained by transfer of parameters from smaller 3 × 3 sheets calculated using DFT at the BPW91/6-31G** level. Red vertical lines represent predicted normal modes and black lineshapes were obtained assuming a 60% Gaussian and 40% Lorentzian line shape function with fwhm of 14 cm^{-1}.

The VCD predicted for parallel structures (Figure 2c) is uniformly negative over the amide I when realistic band shapes are taken into account. By contrast, that for the antiparallel (Figure 2d) is quite weak (5−10 times less intense than parallel for flat sheets) and has a positive couplet shape mostly corresponding to the lower energy absorbance band.[9] In Raman, the parallel (Figure 2e) and antiparallel (Figure 2f) amide I patterns are similar since in both forms the central components, at ∼1670 cm^{-1} in these (vacuum) calculations, correspond to the intense Raman modes.

IR and VCD of modes other than the amide I prove to be less useful for conformational study. The amide II (at ∼1550 cm^{-1} for N-protonated amides) is very similar for parallel and antiparallel structures in both IR and VCD (Figure 2a−d). In Raman (Figure 2e,f), the amide II is very weak and essentially featureless for both β-sheet types. The extended amide III region spanning 1400−1200 cm^{-1}, which contains mixes of C−N stretch with the N−H and C_α−H deformations, is very weak in IR and VCD and consequently of little use for structural studies.[67] Our simulations suggest some sign and intensity variation from 1400 to 1350 cm^{-1}, where a positive VCD couplet is predicted for the parallel sheet, while a negative one is obtained for the antiparallel. Given their weak magnitude, these signals are not likely to be practically useful.

Raman in the amide III region, on the other hand, is believed to be the band most sensitive to conformation.[68] The in-phase combination of the C_α−H bend with the amide III N−H bend creates an intense Raman band centered around ∼1235 cm^{-1}, while the out-of-phase combinations give rise to two weaker bands between 1300 and 1400 cm^{-1}. The smaller peak near 1400 cm^{-1} has a significantly larger contribution from the C_α−H bending. Our simulations predict intensity differences between parallel and antiparallel β-sheets, notably at ∼1330−1300 cm^{-1}, but they probably are not distinctive enough to offer a reliable means for structural discrimination. Moreover, for nonresonance Raman of heteropeptide samples, this region is often overlapped by side-chain bands, which can be minimized by far-UV (amide) resonance excitation.[68,69] By contrast, side chain contributions are much less intense in IR and are normally negligible in VCD.

Twist and Registry Shift. Twisting of the sheet plane, and consequently of the strands, is an important structural variation in real β-sheets but has little effect on the amide I exciton spread. As shown in Figure 3, twisting is predicted to have only a minor impact on the amide I in either IR (Figure 3a,b) or Raman (Figure 3e,f) but does shift the frequency of the amide II up for parallel sheets and down for antiparallel sheets. By contrast, if the strands are out of register, the parallel β-sheet amide I IR intensity distribution changes (Figure 3a), because the non-hydrogen bonded amides (edge and terminal residues) create a weak high frequency component. Misalignment of the strands can therefore cause parallel and antiparallel β-sheet

dx.doi.org/10.1021/jp4056126 | J. Phys. Chem. B XXXX, XXX, XXX−XXX

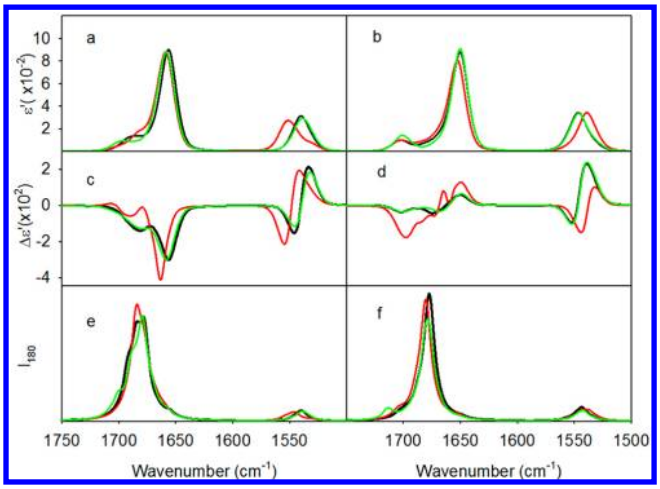

Figure 3. Effects of twist and registry shift on the β-sheet vibrational spectra. Simulated amide I and amide II IR (a and b), VCD (c and d), and Raman (e and f) spectra for parallel (left) and antiparallel (right) model β-sheets with flat geometry and in-register strands (black), twisted geometry and in-register strands (red), and flat geometry and out-of-register strands shifted by one amide (green). The spectra were calculated using the same methods described in Figure 2.

amide I IR to become more alike, making it more difficult to discriminate structural types.

As might be expected, VCD (Figure 3c,d) is more sensitive to the β-sheet twist than to the registry shift. In particular for the antiparallel sheets, the twist causes a significant increase in the amide I VCD intensity. However, the sign patterns, all negative for parallel and couplet for antiparallel, are qualitatively the same as for the planar sheets.

N-Deuteration. IR and VCD spectra are often measured in D_2O-based solutions with N-deuterated amide groups, for which modes are denoted by adding a prime, i.e., amide I′, II′, etc. Since N-deuteration does not offer any additional advantages for structural discrimination, simulated spectra showing its effects are presented in the Supporting Information, Figure S4. The most pronounced effect of the N-deuteration is the shift of the amide II′ band down by ~100 cm^{-1}, with a loss of VCD intensity but a significant gain in Raman intensity. The amide III′ shifts below 1100 cm^{-1} and is no longer coupled to the C_α−H bending modes, which now yield a Raman band just below 1300 cm^{-1} that has negative VCD. Parallel sheets have a distinct Raman band above 1300 cm^{-1} with positive VCD, while antiparallel do not. The amide II′ and III′ are not predicted to be particularly useful for structure determination due to relatively little variance as well as overlap with side-chain and solvent bands in IR and Raman, the latter being less of a problem for VCD. The amide I′ IR shifts slightly lower in frequency with respect to amide I (~4 cm^{-1}) and somewhat more in the Raman, but the shape remains essentially the same in all three types of spectra. The same effects described above for twisting and registry shift are seen for those structures with N-deuteration, as illustrated in Figure S5 in the Supporting Information. Since amide I′ studies in D_2O based solvent predominate and because there are only minor differences from the amide I, from this point on unless noted otherwise, we will present N-deuterated simulations.

Isotopic Labeling. Site specific isotopic labeling of peptides with ^{13}C on the amide carbonyls (C═O) significantly enhances the potential of vibrational spectroscopies to discriminate between different conformations. The greatest effect of ^{13}C labeling is observed for the amide I or I′, resulting in a sideband about 40 cm^{-1} below the main band. A much less shifted ^{13}C sideband is observed for the amide II′ in N-deuterated peptides (Supporting Information, Figure S6), while other amide bands, including the N-protonated amide II (see below), which has a much smaller contribution of the C−N stretch than amide II′, are virtually insensitive to ^{13}C isotopic labeling.

Figure 4 shows simulated amide I′ spectra for model β-sheets singly labeled in each strand at three different positions. For the parallel case (Figure 4a,c,e), the ^{13}C═O sideband is shifted down ~40 cm^{-1} from the intense ^{12}C═O IR band, but somewhat more separation (and less intensity) occurs in Raman due to the difference in ^{12}C intensity distributions (see below). Side bands in parallel IR and Raman are independent of the ^{13}C position in the sequence, aside from terminal groups (not shown). The stable spectral pattern irrespective of the label position develops for parallel sheets because the labels are always in the same relative strand-to-strand arrangement.

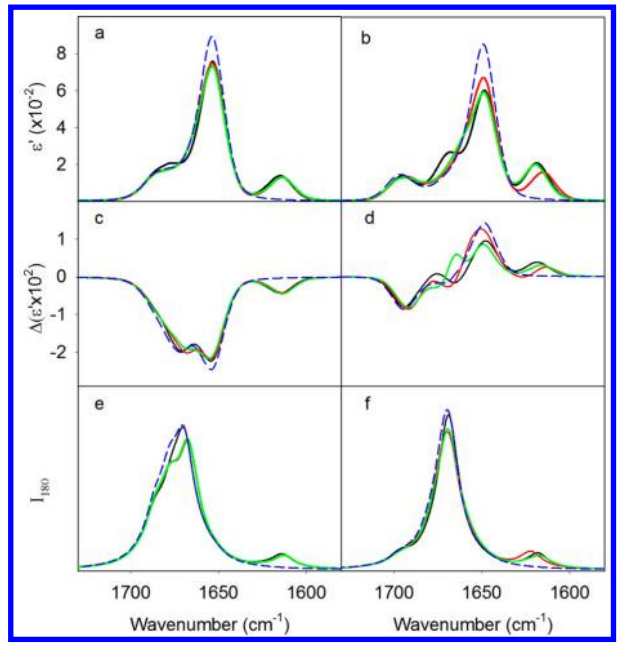

Figure 4. Amide I′ vibrational spectra of isotopically edited β-sheets with single ^{13}C substitutions. Simulated amide I′ IR (a and b), VCD (c and d), and Raman (e and f) spectra for parallel (left) and antiparallel (right) β-sheets with ^{13}C labels on amide 2 (black), amide 5 (green), and amide 6 (red). Unlabeled spectra are shown as dashed blue lines.

For antiparallel sheets, the shift of the ^{13}C═O from the main ^{12}C═O band in the IR (Figure 4b) and VCD (Figure 4d) is predicted to be smaller (30−35 cm^{-1}), unless the isotopic labels are closely aligned between strands as occurs in the parallel sheet. This interaction is maximized for labels on the central residue of in-register antiparallel strands with an odd number of amides, where the ^{13}C labeled amides align across strands in the closest possible proximity. For strands with an even number of amides, such alignment is impossible (Supporting Information, Figure S7). Here, a somewhat smaller but still distinct frequency shift occurs for the $(n/2) + 1$ labeled position (where n, number of amides in the strand, is even), because for this position the labeled amides on neighboring strands are connected through the small H-bond ring (Supporting Information, Figure S7). All the other label positions, including those related via the large H-bond ring,

dx.doi.org/10.1021/jp4056126 | J. Phys. Chem. B XXXX, XXX, XXX−XXX

are predicted to have essentially the same $^{13}C{=}O$ band frequency. For ten amides per strand (n = 10) as used in our models, $(n/2) + 1 = 6$. Therefore, ^{13}C labeled position 6 exhibits a distinctly greater frequency IR shift of the isotopic band than any other position (Figure 4b,d). Since the label alignment changes with register shift, the relative frequency shifts of the different ^{13}C labels near the center of the sequence can be used as a probe of in- or out-of-register strand arrangements in antiparallel β-sheets (Figure S8 in the Supporting Information), and this has been exploited experimentally.[26,32−37] For the parallel sheets, out-of-register strands would still yield a consistent ^{13}C band irrespective of labeling position but would have less frequency shift.

VCD of the ^{13}C labeled β-sheets follows the unlabeled patterns described above, remaining generally negative for parallel and a couplet, low wavenumber positive, for antiparallel. The $^{13}C{=}O$ modes reflect the $^{12}C{=}O$ signs, yielding all negative VCD for parallel, but all positive for antiparallel sheets, as the negative part of the couplet is overlapped by the positive $^{12}C{=}O$ part. This opposite sign for the two sheet types, if detectable, would therefore be a more definitive discriminator of conformation than the IR pattern. The ^{13}C frequency shift is also slightly greater in VCD than for the IR due to the underlying couplet band shape.

In the Raman spectra, the $^{13}C{=}O$ modes are close in frequency to the IR values but the intense $^{12}C{=}O$ modes are higher than the IR, enhancing the apparent separation (see Figure 4 and Figure S6, Supporting Information). For parallel β-sheets, (Figure 4e) the single-label amide I′ Raman spectra are again virtually independent of the label positions. However, for antiparallel sheets, position 6 has a higher frequency $^{13}C{=}O$ band in the Raman than do other positions in the antiparallel alignment (Figure 4f), which is opposite to the IR pattern (Figure 4b). Since there is only one ^{13}C per strand, this difference is symptomatic of interactions leading to differently phased cross-strand coupled modes, shifted in frequency, dominating the observed IR and Raman amide I′ bandshapes (see Figure S9 in the Supporting Information). The frequency differences between the ^{13}C antiparallel positions are also smaller in Raman than in the IR, which combined with weaker ^{13}C intensities and side-chain interference, may limit practical applications for discriminating between β-sheet structural types.

With double ^{13}C labeling, other distinctive features arise between conformers, as shown in Figure 5. If two labeled sites are placed adjacent to each other (sequential), then a somewhat more intense IR $^{13}C{=}O$ band appears shifted down as compared to the single labels for both parallel and antiparallel structures. The sensitivity of adjacent labels to structure arises from their cross-strand positions which results in maximum shifts for labels on the two central amides (5 and 6 in this model) in exact analogy to the single labeling patterns (Figures S7 and S8 in the Supporting Information). However, if the labeled positions are separated by one residue (alternate in sequence) and on one side of the center residue, then in both structures the frequency shifts up, but for the antiparallel case the $^{13}C{=}O$ band gains more intensity in the IR, with a more than compensating loss in the main $^{12}C{=}O$ band (Figure 5a,b).[38,39] Alternate double labeling therefore provides a unique conformational test that is not dependent on the frequency change for the antiparallel sheet (Figure 5b) but rather the intensity gain (and loss in the unlabeled $^{12}C{=}O$) which is much less for parallel sheets (Figure 5a). This difference in sequential and alternate label frequency shifts is due to the

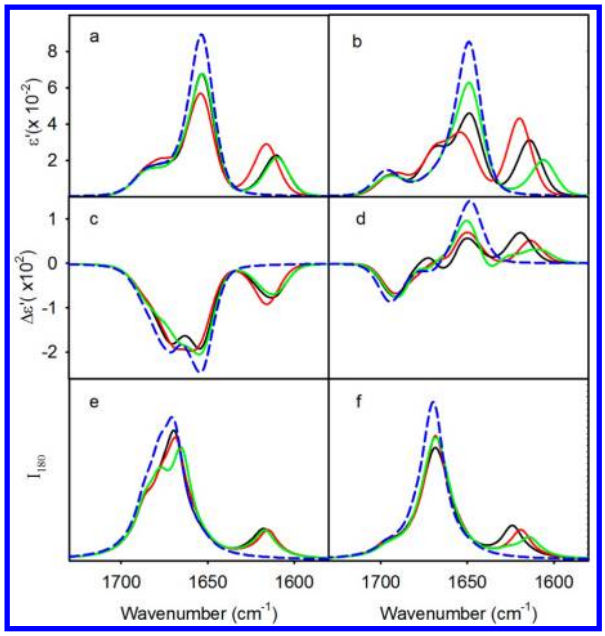

Figure 5. Amide I′ vibrational spectra of isotopically edited β-sheets with double ^{13}C substitutions. Simulated amide I′ IR (a and b), VCD (c and d), and Raman (e and f) spectra for parallel (left) and antiparallel (right) β-sheets with labels at positions 2 and 3 (black), 2 and 4 (red), and 5 and 6 (green). Unlabeled spectra are shown as dashed blue lines.

opposite sign of the in-strand coupling constant, making the upper (alternate) or lower (sequential) ^{13}C component more intense.

The $^{13}C{=}O$ VCD for doubly labeled parallel sheets is again negative and essentially follows the IR signal in both frequency and intensity (Figure 5c). For antiparallel sheets (Figure 5d), while the $^{13}C{=}O$ VCD remains positive as in single labeled sheets, the maxima in relation to the IR depend on the labeling position. For sequentially labeled amides, the VCD peaks to the high frequency side of the IR maximum, while for alternate labels (at positions 2 and 4) it is the opposite. Furthermore, sequential labels in positions 5 and 6, which exhibit unique interstrand coupling (Figures S7 and S8 in the Supporting Information), result in a broader $^{13}C{=}O$ VCD band shape.

Double isotopic labels in Raman spectra (Figure 5e,f) qualitatively follow the single label predictions shown above (Figure 4). However, sequential (for example, positions 2, 3) and alternate (2, 4) ^{13}C labels have opposite relative positions in Raman (higher and lower in frequency, respectively) than in the IR (Figure 5d,f). Because of stronger $^{13}C{=}O$ signals and more pronounced frequency shifts in the antiparallel sheets (Figure 5f), double isotopic labeling appears to be the only practical means for distinguishing between β-sheet structures with Raman.

Considering other modes, for the N-protonated case, there are only small isotope effects (a broadened shoulder to low frequency) predicted for the amide II (Figure S10, Supporting Information). Since there was no obvious effect on amide III (~1240 and 1370 cm^{-1} bands, N−H and C_α−H bends mixed) those data are not shown. However, for the N-deuterated peptides (Figure 6), the amide II′ has a potentially detectable ^{13}C sideband, shifted down by ~15 cm^{-1} from the main amide II′ intensity in both the Raman and IR spectra. Although the labeled amide II′ predictions differ for parallel and antiparallel

dx.doi.org/10.1021/jp4056126 | J. Phys. Chem. B XXXX, XXX, XXX−XXX

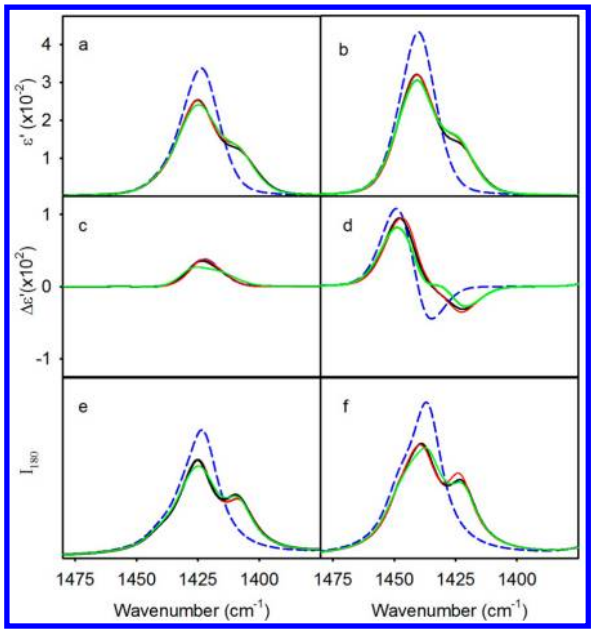

Figure 6. Amide II′ vibrational spectra of isotopically edited β-sheets with double ^{13}C substitutions on two consecutive amides. Simulated IR (a and b), VCD (c and d), and Raman (e and f) spectra for parallel (left) and antiparallel (right) sheets with labels at positions 2 and 3 (black), 4 and 6 (red), and 5 and 6 (green). Unlabeled spectra are shown as dashed blue lines.

sheets, the differences are probably too small for reliable detection. Additionally, overlap of $-CH_2$ and $-CH_3$ modes from side-chains, and HOD from the solvent, is likely to make isotope effects on this band only marginally useful.

We have also calculated spectra for ^{13}C labeled and unlabeled twisted parallel and antiparallel sheets, for which selected results are provided in Figures S11 and S12, Supporting Information. As expected from the unlabeled results (Figure 3), the isotope labeled, twisted sheets develop the same overall patterns as seen for flat sheets (Figures 4 and 5) with relatively minor variations. The biggest changes due to twisting are for the VCD spectra, which are uniquely sensitive to chirality. For parallel sheets, despite more variation in band shape, a mostly negative overall amide I′ VCD still results (Figures S11 and S12 in the Supporting Information). For antiparallel sheets, more intense amide I′ VCD with an overall couplet shape is predicted for twisted sheets with single and sequential double labels as was seen above for flat sheets (Figures 4 and 5). However, more significant differences are computed for sheets with alternating double labels, resulting in more pronounced couplet signals in the $^{13}C{=}O$ band, positive to the low frequency (Figure S12 in the Supporting Information). These observations suggest that selected double ^{13}C substitutions may be useful for sorting out parallel and antiparallel sheets and, in combination with VCD, for monitoring the degree of (isolated) sheet twist.

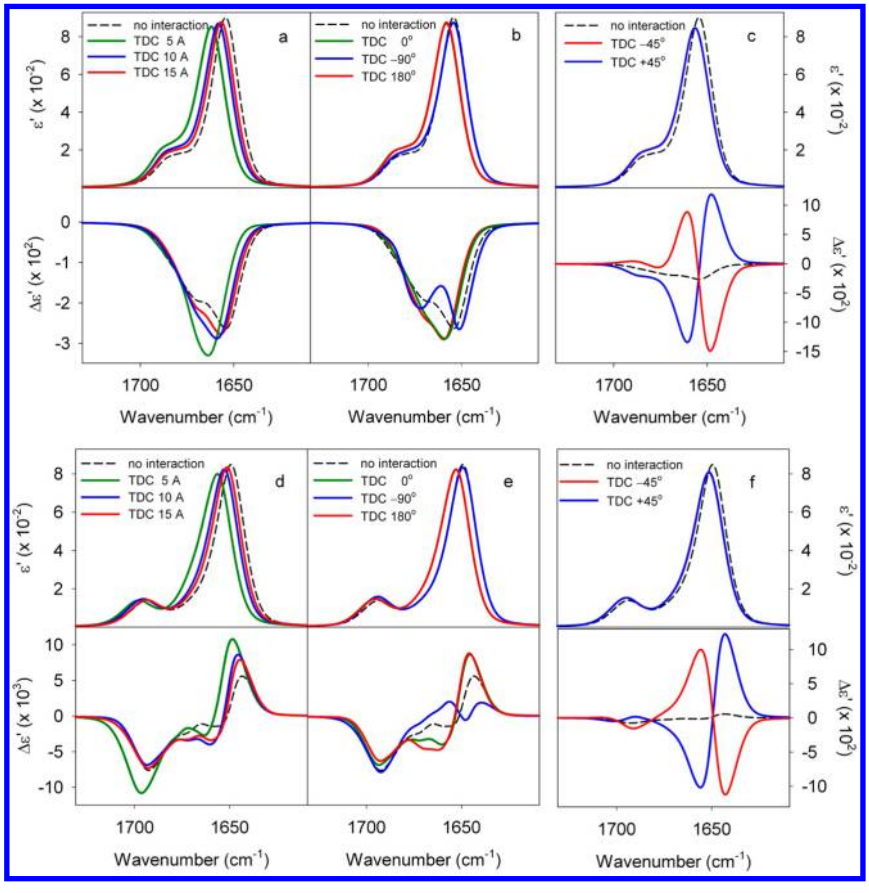

Figure 7. Amide I′ IR and VCD spectra for stacked, flat β-sheet structures. The spectra were calculated using transfer of DFT parameters and TDC approximation for intersheet coupling for two stacked β-sheets with both parallel (a–c) and antiparallel (d–f) strands. Distance (a, d) dependence is calculated for the 0° orientation and 5, 10, and 15 Å between the sheets. The comparisons of 0, −90, and 180° (b, e) and ±45° (c, f) relative sheet orientations are calculated for the 10 Å intersheet separation.

dx.doi.org/10.1021/jp4056126 | J. Phys. Chem. B XXXX, XXX, XXX–XXX

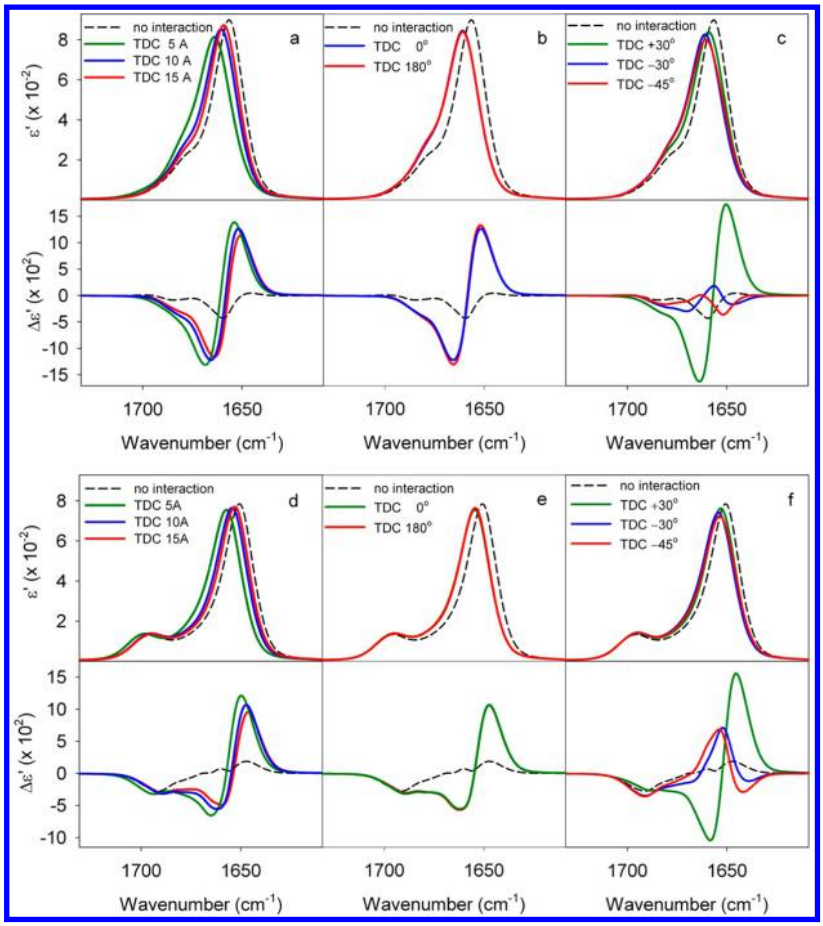

Figure 8. Amide I′ IR and VCD spectra for stacked, twisted β-sheet structures. The spectra were calculated using transfer of DFT parameters and TDC approximation for intersheet coupling for two stacked β-sheets with both parallel (a–c) and antiparallel (d–f) strands. Distance (a, d) dependence is calculated for the 0° orientation and 5, 10, and 15 Å between the sheets. The 0 and 180° (b, e) and +30, −30, and −45 (c, f) orientations are calculated for the 10 Å intersheet separation.

Stacked Sheets. Stacking of two or more β-sheets occurs in structures such as amyloid fibrils and likely also in insoluble peptide and protein aggregates. The stacked sheets may align in either parallel or antiparallel manner or even at an angle[7,8,16,17] potentially resulting in spiral structures.[70−73] Simulations of the spectra for stacks of sheets using the DFT and transfer methodology would not only require DFT calculations on much larger structures, but the variety of possible arrangements would also necessitate many separate DFT computations. Therefore, to make these calculations tractable, the longer-range, intersheet interactions were approximated by TDC, as described in Methods. To verify that TDC is a reasonable approximation, it was first tested against full DFT calculations for a smaller system, which demonstrate that TDC is indeed a good approximation for the through space, intersheet vibrational couplings (Figure S13, Supporting Information). While some differences between the full DFT and the TDC model can be observed in VCD, the qualitative patterns and even overall quantitative signal strengths are reproduced very well.

On the basis of these tests, we have carried out more extensive computations of spectra for multiple sheets using TDC for intersheet coupling. The major variables to model are the intersheet spacing and the relative orientation of the two sheets (Figure 1). Simulations for two stacked, five-stranded sheets with ten amides per strand, both parallel and antiparallel and with varying intersheet distance and orientation are shown in Figure 7. On decrease of intersheet spacing, the major change is a shift of the intense low frequency component to a higher wavenumber, but the general shape is maintained (Figure 7a,d). For testing of other intersheet orientations, we chose a 1 nm separation as a value that might be appropriate for intersheet stacking separations in fibril structures.[7,8,16,17] To denote the geometries here, in order to avoid confusion with parallel and antiparallel arrangement of the strands in a single sheet, we use the angle between the strand axes of the neighboring stacked sheets (Figure 1). Variation of the angle between two sheets has relatively little impact on the IR spectral shapes but does shift the frequencies somewhat. The amide I′ for 0° (each sheet the same orientation) and 180° (pairwise oppositely oriented) structures are predicted to be virtually the same and shifted higher than those for sheets at right angles to each other (±90°). The latter have spectra nearly indistinguishable from two noninteracting sheets. This is consistent with dipole coupling effects, which are expected to be maximal when aligned and minimal when perpendicular.

The VCD for the stacked sheets that are aligned (0°), opposite (180°), or perpendicular (±90°) show the same qualitative patterns as seen for noninteracting sheets, with only very minor differences due to varying distance and orientation. By contrast, those for sheets twisted to ±45° relative orientations exhibit a huge intensity enhancement, about a factor of twenty for antiparallel and five for parallel sheets

dx.doi.org/10.1021/jp4056126 | J. Phys. Chem. B XXXX, XXX, XXX−XXX

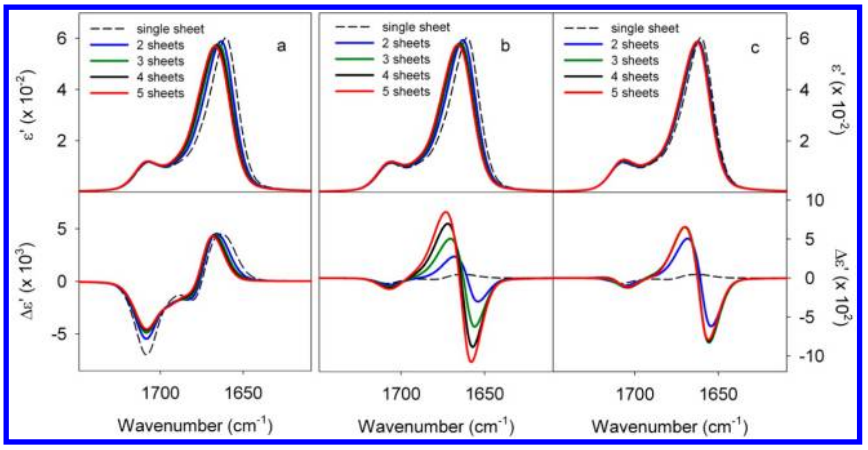

Figure 9. Effect of the number of stacked sheets on the amide I′ IR and VCD spectra for flat, antiparallel sheets. Simulated spectra for two to five stacked antiparallel, flat β-sheets (five strands of five amides each) in 0° orientation (a), −15° orientation (b), and −45° orientation (c) are shown. The spectra were calculated by the transfer of DFT vibrational parameters on the individual sheets and using TDC approximation for intersheet coupling.

(Figure 7c,f). These large VCD intensities are obviously due to the intersheet interactions and, as expected, yield essentially mirror-image VCD spectra for the left (−45°) and right (+45°) handed rotations. This suggests that VCD could be a very sensitive probe of stacked β-sheet structures where the individual sheets deviate from either type of aligned orientation. On the other hand, for randomly assembled aggregates, or ones where the sheet-to-sheet orientations deviate in both angular variants, essentially a racemic mixture would be produced with negligible effect on the VCD. Furthermore, the sign pattern of the enhanced VCD is the same for either parallel or antiparallel (strand alignment) sheets, since the coupling depends only on the relative rotational orientation of the sheet oscillators. Thus, observation of a couplet VCD for a fibrillar or aggregated sheet assembly would not be diagnostic of the underlying sheet type.

Dramatically enhanced VCD has been seen in various fibrillar protein and peptide systems that have also been shown to have twisted structures.[17,18,70−72] For this reason, we further investigated the effects of the stacking of twisted β-sheets, as shown in Figure 8. Here, unlike for the flat sheets, significant VCD enhancement is observed for the 0° orientations, i.e., sheets aligned in the same direction. A relatively slow loss of VCD intensity (and slight reduction in exciton width) occurs with increasing distance between the sheets. For both parallel and antiparallel twisted sheets, the enhanced amide I′ VCD due to stacking is a positive couplet. However, for parallel sheets the couplet is nearly conservative (approximately equal positive and negative intensities), while the antiparallel sheet exhibits a discernible positive bias (more intense positive intensity, with the negative lobe spread over the exciton dispersion). Despite the similar overall shape, these qualitative differences may be useful for the discrimination between the two strand arrangements.[74]

With oppositely aligned sheets (180°) the spectra are virtually identical to the 0°, again with a significant enhancement in the VCD (Figure 8b,e). Relative orientation of the twisted sheets other than 0° or 180° can further influence the VCD signal, depending on the sense of the intersheet rotation (Figure 8c,f). The left-handed rotation (e.g., −30°) results in weaker VCD, while the right-handed (+30°) one yields additional VCD enhancement. Qualitatively, this can be explained as an additive effect of the two different VCD mechanisms: one arising from the sheet twist and the other from the relative sheet orientation (induced helicity) as seen above for flat sheets (Figure 7c,f). The former is always a positive couplet, while the latter is negative for left-handed (e.g., −30°) leading to partial cancellation and positive for the right-handed (e.g., +30°) orientation, causing an additional intensity enhancement. More drastic intersheet rotations, as tested above for flat sheets, such as +45° and ±90°, do not appear to be sterically reasonable for twisted sheet geometries and were not investigated.

For twisted sheets, unlike the flat ones, the IR and VCD are much more sensitive to the β-strand lengths. The effects of strand length as well as number of strands per sheet on the IR and VCD of stacked, twisted sheets are illustrated in Figure S14, Supporting Information. Long strands generally result in a narrower amide I′ IR and greater enhancement of the VCD. By contrast, greater number of strands increases the IR exciton dispersion but has very little effect on the VCD intensity. This might be expected from the increased coupling in the strand, leading to a sharper low frequency amide I′ component in both sheets, whose dipolar coupling could be the source of the enhanced VCD.

Stacking introduces an additional structural dimension, for which we examine the effects of increasing the number of stacked sheets. In Figure 9, the simulated IR and VCD spectra are shown for stacked structures containing two to five antiparallel, five stranded sheets in 0°, −15°, and −45° relative orientations. Shorter peptide strands of only five amides were used to allow simulations of up to five stacked sheets.

For the 0° oriented stacked sheets (Figure 9a), the IR amide I′ shifts higher in frequency and loses a small amount of intensity (per amide group) with increase in the number of sheets, though the incremental change converges by four stacked sheets. The VCD also shows little change for the largest stack. For the −15° oriented sheets (Figure 9b), the IR is very similar to that of 0°. However the VCD grows significantly (note the different scale from Figure 9a), the signal increasing nearly linearly with the number of strands up to four, with the increment decreasing for the fifth sheet, which suggests a slow leveling off. By contrast, for the −45° oriented sheets, the most significant change is from one to two sheets, after which the IR stays virtually constant and only minor enhancement is seen in VCD due to adding the third sheet, beyond which there is no further increase. While for two stacked sheets the −45°

dx.doi.org/10.1021/jp4056126 | J. Phys. Chem. B XXXX, XXX, XXX−XXX

orientation has the strongest VCD, for 5 and even 4 sheets the −15° orientation between sheets gives more intensity. This can be intuitively understood from the fact that for the −45° oriented neighboring sheets, the relative orientation of the first and third is −90° giving no further enhancement (Figure 8). The general trend is that the VCD is expected to grow until the angle between the first and last sheet in the stacked structure reaches ±90°.

The VCD enhancement due to multiple stacking was investigated on twisted sheet models with longer (ten amide) strands (Figure 10) as well as shorter (five amide) strands

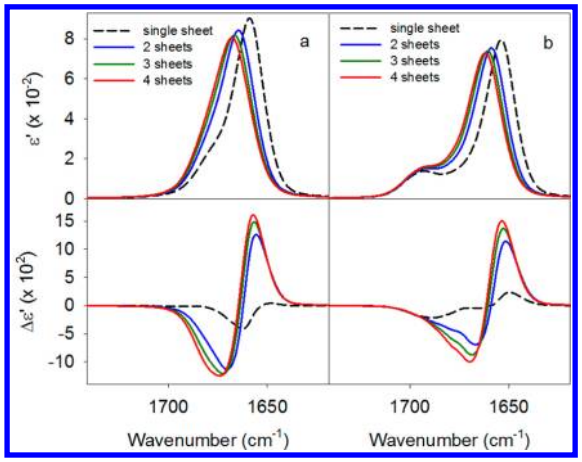

Figure 10. Effect of the number of stacked sheets on the amide I′ IR and VCD spectra for twisted, parallel, and antiparallel sheets. Simulated amide I′ IR and VCD for two to five stacked parallel (a) and antiparallel (b), twisted β-sheets (three strands of ten amides each) in 0° orientation, simulated by the transfer of DFT vibrational parameters on the individual sheets and using TDC approximation for intersheet coupling.

(Supporting Information, Figure S15). For the longer strand models (Figure 10) the VCD signal does increase with the number of sheets in the stacked structure; however, the increase with no relative rotation between sheets is relatively modest, about 13% (peak to peak) from two to three sheets, and somewhat less (~11%) when the fourth sheet is added. The exciton width of the amide I′ also contracts with an increasing number of sheets, as seen above for the smaller flat sheets (Figure 9) as well as twisted ones (Figure S15, Supporting Information) and as most evident from the shift of the IR maximum. For the sheets composed of five amide strands (Figure S15 in the Supporting Information), the VCD intensity enhancement is much weaker and the amide I′ shift is smaller.

Isotope labels in stacked sheets have virtually the same impact on IR and VCD spectra as seen for single sheets (see Figures S16 and S17, Supporting Information). The IR closely resembles that for single sheets in both parallel and antiparallel cases, and the isotope shifts remain consistent with the single sheet results noted above, with the central residues having shifts sensitive to antiparallel registry and the alternate labels having enhanced intensity. VCD for ^{12}C═O modes in flat stacked parallel sheets, aligned at 0°, remains predominantly negative, while that for antiparallel sheets has an overall couplet pattern but becomes more complex, probably due to the coupling of more oscillators. Rotating the sheets again leads to intense couplet VCD. The ^{13}C═O VCD band in isotopically labeled stacked sheets again essentially follows the sign of the lower frequency ^{12}C═O VCD component, with aligned (0°) parallel being negative and antiparallel positive. These trends fit the stacking of twisted sheets as well, but now the ^{13}C═O VCD band is positive for both since both have the same sense of ^{12}C═O couplet (Figures S18 and S19, Supporting Information).

DISCUSSION

Structural Characterization of β-Sheets with Vibrational Spectroscopies. Significant effort has been devoted to understanding the β-sheet structure, particularly in the context of protein aggregation and fibril formation. Vibrational spectroscopic techniques, such as IR, VCD, and Raman spectroscopies, have been widely used to probe the details of the β-sheet arrangements in model peptide and protein fibrils. However, because of the size and complexity of such structures, it is not straightforward to interpret the experimental spectra in terms of the structure. For this reason, theoretical simulations of the vibrational spectra of model compounds, which can be directly compared with experiment, have become indispensable. Here we have shown that DFT-based simulations of β-sheet spectra predict distinct IR, VCD, and Raman intensity patterns for parallel and antiparallel sheet structures. A summary of our predictive results with these spectral simulations is provided in Table 1. While these are similar to earlier predictions of differentiation for these conformers based on amide I/I′ IR,[9−15] our data explicitly show those patterns arise from differences in intensity distribution over the exciton dispersion of component modes. Furthermore we show that these variations are moderated by twisting and out of register sheet formation. In the absence of intersheet stacking, these conformers are most clearly discriminated by VCD band shape, assuming it is measurable, since the parallel structure is predicted to have predominantly negative VCD and the antiparallel an overall couplet shape, positive to low wavenumber, in the amide I region. However, this pattern can be overwhelmed by stacking effects, which may be more important in determining the VCD spectra of real β-sheet conformations.

In addition to IR and VCD, we have also identified potentially useful signatures of different β-sheet structures in Raman spectroscopy. In particular, frequency and intensity differences in the 1050−1450 cm^{-1} region are of interest since these are not easily accessible to IR and VCD measurements in aqueous solution. However for real systems with heterogeneous sequences, the Raman in this region will also have significant interference from intense bands originating in the side-chains, which were not included in these Ala-peptide simulations.

If the strands are isotopically labeled, additional structural tools become available with vibrational spectroscopy. Single labels placed in parallel structures have virtually the same effect on the spectral pattern, for all positions in the sequence (aside from termini). On the other hand, in antiparallel sheets the ^{13}C═O band varies with sequence position, which has motivated previous labeling studies on aggregate or fibril forming peptides.[26,32−37] Labels near the centers of strands in register will lead to a significantly larger isotope shift than for other sequence positions; however, using absolute shifts for analysis of an isolated label in the sequence is experimentally difficult (for examples, see the following accompanying paper[62]). By comparing relative shifts for labels placed in different sequence positions, previous workers have postulated that several short oligopeptides assembled into antiparallel

dx.doi.org/10.1021/jp4056126 | J. Phys. Chem. B XXXX, XXX, XXX−XXX

Table 1. Overview of the Main Vibrational Spectral Signatures Suitable for Discrimination among Specific β-Sheet Structural Features

structural feature	method	spectral signatures	comments
parallel vs antiparallel	IR	amide I/I′ band shape: narrower for parallel; greater apparent splitting for antiparallel sheets	predominantly for planar in-register sheets, distinction diminished with twist and registry shift
	IR with ^{13}C editing	^{13}C amide I/I′: independent of label position in parallel sheets; distinct frequencies and intensities depending on label positions in antiparallel sheets	unique frequency shifts for ^{13}C labels in alignment and small H-bonded rings.
			^{13}C intensity enhancement for off-center alternate double labels
	VCD	amide I/I′ sign: negative for parallel, positive couplet for antiparallel sheets	single sheets without intersheet stacking.
			very weak VCD for flat sheets, stronger for twisted structures
	VCD with ^{13}C editing	^{13}C amide I/I′: sign and position with respect to the IR maximum	variation in relative IR/VCD peak positions for doubly labeled peptides
	Raman with ^{13}C editing	^{13}C amide I/I′: independent of label position in parallel sheets; distinct frequencies and intensities depending on label positions in antiparallel sheets	Raman without ^{13}C labeling not sufficient for reliable discrimination
			double labeling preferred: single ^{13}C labeling may not provide enough distinction
			different frequency shifts and intensity patterns with label positions than in IR
β-sheet twist	VCD	amide I/I′: stronger VCD compared to flat sheets.	particularly for antiparallel sheets. Same sign patterns (parallel and antiparallel) as for flat sheets
register alignment	IR with ^{13}C editing	^{13}C amide I/I′: frequency shifts and intensity variations depending on the relative label positions	detailed strand alignment in antiparallel sheets. In parallel sheets same ^{13}C frequency if in exact register or not
	VCD with ^{13}C editing	^{13}C amide I/I′: peak position with respect to the IR maximum	
	Raman with ^{13}C editing	^{13}C amide I/I′: distinct frequency shifts depending on label positions	double labeling may be necessary
			detailed strand alignment in antiparallel sheets. In parallel sheets only if in exact register or not
sheet stacking	VCD including ^{13}C editing	amide I/I′: Significant VCD intensity enhancements	minor effects on IR and Raman.
		intense couplet shapes for both parallel and antiparallel sheets	planar sheets: sign depends on the intersheet orientation
			twisted sheets: positive couplet shapes. Difference in relative positive/negative VCD intensities for parallel and antiparallel sheets

sheets upon aggregation or fibrilization since frequencies and intensities for peptides labeled on the center residues shifted significantly from those labeled earlier or later in the sequence.[32−37] In principle, these studies can also determine the degree to which strands are out of register.[33,34] In the following paper,[62] we apply these spectral simulation methods directly to specific peptide models for which multiple singly labeled ^{13}C isotopologues were synthesized and their aggregates studied experimentally by IR[32−36] and VCD.[35] There we show that a consistent picture of the arrangements of the β-strands can be obtained from the ^{13}C amide I IR and VCD spectra.

Double labeling of alternate residues, particularly if they are located on one or the other side of the strand center, can lead to a large intensity enhancement of the ^{13}C═O band and large loss of the ^{12}C═O band intensity that consequently provides a unique diagnostic for antiparallel structures. This sort of pattern has been seen experimentally in labeled peptides studied by Brauner and Mendelsohn and confirmed by DFT-based modeling of ideal sheets.[9,38] More recently, we have made peptides rich in glutamic acid with interspersed labeled Val residues that again have a maximum amide I′ intensity in the ^{13}C═O component when two labels were placed in alternate positions.[74]

Comparison to Alternate Simulation Methods. A number of previous reports have modeled β-sheet vibrational spectra theoretically using various methods. The majority of theoretical studies focused on the amide I IR, with far fewer attempts to simulate the VCD or Raman spectra. Most previous models approached this as an extension of historically accepted empirical or classical methods, which viewed the peptides as collections of identical oscillators with different types and extents of coupling represented at various levels of accuracy. Transition dipole coupling (TDC) is the simplest to implement, which has led to its widespread use to account for vibrational couplings of all but the nearest neighbor amide groups.[13,15−17,75] The neighboring amide couplings are treated either empirically[18,38] or via "coupling maps" based on quantum mechanical calculations on small peptide fragments,[11,12] while using TDC[20,21,23] or, alternatively, the more general transition charge coupling[22,32] for longer range interactions.

However, such models, since they arbitrarily select couplings to include, can leave out important local interactions that are fully accounted for in the atomic force field (FF), such as that computed with a quantum mechanical (QM) model.[49,52] In fact, a number of QM calculations have indicated that TDC is inadequate or, at least significantly different from full quantum mechanical couplings, even for more distant amide oscillators. Kubelka et al.[55] showed for a number of different secondary structures that IR absorption patterns predicted by DFT were not well approximated by using TDC coupling constructed from the DFT transition dipoles. Viswanathan and Dannenberg,[76] also using DFT, concluded that TDC cannot be the dominant mechanism responsible for excitonic splitting in β-sheets but that through H-bond coupling is the more important mechanism. Similarly, by a quantum-classical hybrid method, Polzi et al.[77] determined that the splitting of the amide I IR signal results from local through-bond coupling. One consequence of using DFT-computed couplings may be that calculated modes associated with labeled amides are truly dominated by the local contributions of the ^{13}C═O groups, in

dx.doi.org/10.1021/jp4056126 | J. Phys. Chem. B XXXX, XXX, XXX−XXX

contrast to significant coupling with the $^{12}C{=}O$ modes predicted by Brauner et al.,[38] who used unrealistically large magnitudes for the vibrational coupling constants to fit the observed intensity distributions.[32,55]

The assumption of equivalent uncoupled oscillators may also be a source of inconsistency introduced by the commonly used empirical methods. For example, as we demonstrate more in detail in the accompanying paper,[62] we observe much smaller isotopic shifts for labels placed on C-terminal amides than those for N-terminal or inner ones. This is due to the different environment experienced by the C-terminal amide (an "internal field" as termed by Cho[78]) that makes these oscillators nonequivalent. We observe this effect in other structures as well, for example, N- and C-terminal amide groups in α-helices.[58] As a consequence, isotopic labeling at different positions, in particular the termini, produces different isotopic shifts, as consistent with experimental observations.[25] By contrast, treating all amide groups as being equivalent and assigning an arbitrary shift to low frequency for any ^{13}C labeled amide group[32] independent of its sequence position, may lead to incorrectly predicted isotopic spectra. Such arbitrary parameters are not needed in our DFT-based approach.

For VCD spectroscopy, where the coupling is no longer a small perturbation but rather is the origin of the entire VCD signal, the coupled oscillator approximation is even less reliable than for the IR. Bouř and Keiderling[79] demonstrated that the dipole coupling approximation is not adequate and gives qualitatively wrong predictions for the amide I VCD band for some peptide conformations. In particular, the normally weak VCD of β-sheets[9] is very difficult to predict. The DFT/CCT method used here[50] gives a very consistent picture for amide I VCD calculations, showing that isolated parallel β-sheets, even if twisted, have a negative VCD and antiparallel sheets produce a couplet.

On the other hand, in the present study we found TDC to provide an adequate model for long-range intersheet vibrational couplings in stacked sheets, especially for IR simulations. This suggests that TDC is indeed a reasonable model for through-space interaction, even though the full DFT calculation is significantly better for bonded (and H-bonded) couplings. As a consequence, our IR amide I′ simulations of multiple stacked β-sheets parallel the TDC based predictions of Barth and co-workers.[16] For VCD, the agreement of the TDC coupling model with the full DFT calculation is somewhat worse, but our test calculations imply that it is sufficient to predict overall spectral bandshapes, the magnitudes of VCD intensities, and the expected dependence on orientations of the stacked sheets.

VCD Enhancement in Fibrillar Structures. Fibrils composed of local β-sheet layers have been shown to have enhanced VCD experimentally,[17,18,35,70,71] and in our model, we predict two distinct origins for such an increase in VCD intensity. First, for flat sheets, the enhancement is observed only when the sheets are rotated about their norm with respect to each other, so that the maximum VCD intensity occurs for the $\pm 45°$ orientation of two stacked sheets, as would be consistent with a coupled oscillator model of VCD. For a structure composed of more stacked sheets, VCD intensity grows to an even greater extent for successive rotations of smaller relative angles. This enhancement is intuitively easy to understand, since the rotation of the β-sheet planes (in flat sheets) breaks the mirror symmetry and induces chirality (adds helical handedness to the dipole coupling) between sheets.

Second, for twisted sheets, stacking leads to a significant enhancement of the VCD, which is quite intense even for (nonrotated) aligned (0°) or opposite (180°) orientation. For both the parallel and antiparallel cases, stacked twisted β-sheets have similar VCD: an intense positive couplet associated with the lower frequency, strong dipolar component of the IR, which is most commonly observed experimentally in fibril samples.[17,18,35,70−72] The sign of this VCD couplet correlates with the overall right-handed twist of the sheets in the stack, and its enhancement upon stacking arises from effectively creating a coiled-coil like superstructure. Rotating the twisted sheets with respect to each other either further increases or decreases the VCD enhancement, if the sense of the rotation is right- or left-handed, respectively. The intersheet rotation in twisted sheets effectively introduces a second helical axis, whose impact on the summed rotational strengths is either constructive (further enhancing VCD if right-handed) or destructive (decreasing VCD if left-handed). It should be noted, however, that twisted sheets rotated with respect to each other in either direction, but particularly in the right-handed sense, would likely be energetically disfavored. Rotation in either direction necessarily results in nonuniform intersheet distances, i.e., the sheet faces are not in the same contact everywhere. This may negatively affect the stacking interactions, although the details would be of course dependent on the sequence. For the right-handed rotations the distance becomes greater between the sheet centers, while the ends are closer and for some orientations even sterically clash. The left-handed orientations keep the centers close together while the ends diverge, which is more feasible, but overall the 0° or 180° orientations in twisted sheets appear preferable.

For twisted sheets the enhancement due to stacking is also strongly dependent on the length of the β-strand, being much smaller for peptides with five amides per strand than for longer ones with ten amides (Supporting Information, Figure S14). On the other hand, increasing the number of strands (beyond about five) in the β-sheet has no effect on the VCD enhancement (Figure 10 and Supporting Information, Figures S14 and S15). The sensitivity to the strand length may be important, as many model amyloid fibrils studied are formed from short peptide fragments, while biomedically relevant fibrils can, by contrast, be formed by quite long and extended strands either from single protein sequences or coupled peptide segments.[7,8,35,80]

Our stacked sheet simulation results are similar to those obtained by Measey and Schweitzer-Stenner[17,18] based on dipole-coupling simulations. They concluded that enhanced couplet-like VCD is observed in parallel sheets stacked at 0° orientation, provided the sheets are twisted. However, while not completely clear from the model, it appears the coupled oscillator arrays they used (two oscillators per strand, up to 20 strands per sheet) correspond to very different geometries than our structures. For such a hypothetical sheet, we would predict very little enhancement, since the strength of the VCD signal is shown to increase strongly with the strand length due to development of a more uniform exciton coupling both in and between strands (Figures S14 and S15 in the Supporting Information). This, consistent with our previous investigation of TDC,[55] underlines the point that simple oscillator coupling schemes are incomplete approximations, particularly for bonded interactions.

Unlike Measey and Schweitzer-Stenner,[18] we do not predict dramatic differences in the intensities depending on whether

dx.doi.org/10.1021/jp4056126 | J. Phys. Chem. B XXXX, XXX, XXX−XXX

the β-sheets are parallel or antiparallel and/or the stacked sheets are aligned or opposite (0° or 180° in our notation for the sheets). Furthermore, as expected from normal continuity considerations, in our simulations the interactions weaken with the distance between the sheets, yielding weaker VCD at larger separations (Figure 8), while Measey and Schweitzer-Stenner surprisingly report a nonphysical increase in the VCD enhancement with distance.[18] We have also examined the dependence of VCD enhancements, as well as of the IR, on the number of β-sheets in the stacked superstructure, which has not been investigated before. Finally, we predict IR, VCD, and Raman spectra for a variety of other amide modes in all these structural types.

Intense VCD couplets have been observed in insulin fibrils and other protein and peptide fibrillar samples and have been attributed to supermolecular chirality.[70,71,74] Interestingly, oppositely signed couplets were measured for insulin fibrils prepared in different ways, which suggest opposite superhelical twist of the cross-β structure with respect to the fibril axis, there termed "normal" and "reverse" fibrils. These phenomena relate to macrostructures that are differentiated in atomic force microscopy (AFM) and electron microscopy (EM) analyses and seem to be size and aggregation state dependent. As such, the relationship of these enhanced VCD spectra to molecular parameters is unclear and could be due to a twist in the sheet or in the stack, the latter being easier to imagine as the basis for a supermolecular difference, but these are not exclusionary. This illustrates the importance of the chirality and methods such as VCD for gaining insights into fibril formation and structure.

While the aim of this study was to illustrate characteristic vibrational spectral signatures using simple β-sheet models, fine structural details may be an important factors in shaping the experimental spectra. This is encouraging, since it suggests that vibrational spectroscopic methods, especially in combination with site-specific isotopic editing, may be sensitive to very subtle structural variations in the β-sheet aggregates and fibrils.

CONCLUSION

Through simulations of the vibrational spectra for various model β-sheet structures, we examined the spectral signatures that can be expected to serve as experimental markers of different β-sheet conformations. While vibrational spectroscopic techniques alone cannot provide enough information to uniquely solve the structures, they can nevertheless help decide the validity or invalidity of a model structure. We have shown that characteristic amide I/I′ band shape features in IR and Raman can be used to distinguish antiparallel from parallel β-sheets, although they may be obscured by the sheet twist. VCD spectra can provide distinct sign patterns, although they may have little intensity, especially for large flat sheets. Twisting of the β-sheet plane leads to a slight enhancement of the VCD signal for isolated sheets, but sheet stacking can significantly enhance the VCD, up to an order of magnitude. In flat sheets the VCD enhancement is entirely due to the superhelicity induced by the mutual orientation (rotation) of the individual sheets, whose sense can be deduced from the sign of the VCD couplet. In twisted β-sheets the VCD is enhanced due to helicity along the strand axis, even for aligned sheets. Both parallel and antiparallel sheets have similar positive couplet amide I VCD due to the same sense of sheet twist. However, the sheet rotation, if present, can either further strengthen or partially cancel the VCD depending on the orientation. The degree of the enhancement in twisted sheets is also sensitive to the length of the β-strands.

The most sensitive probe of the strand arrangement is ^{13}C isotopic editing, as observed with the amide I′ band, in particular if several distinct sites in the peptide or protein are labeled. Furthermore, double labeling can significantly enhance the isotopic signals depending on the label position, which provides yet another important spectral signature correlated to structure. However, the particular spectral patterns are difficult to predict or interpret without the theoretical simulation of the spectra. In this respect, the quantum mechanical DFT calculations, combined with the parameter transfer, provide important, independent means for identifying the expected experimental spectral features arising from particular structures. These are free of arbitrary parameters used to fit spectra with empirical models. In addition, such simulations can be used to help design experimental approaches, such as ^{13}C labeling schemes to specifically distinguish between particular β-sheet arrangements.

Finally, the nonempirical nature of our models provides an important test for other methods, such as simplified, empirical coupled oscillator models. While valuable, in particular due to their computational efficiency, these approaches nevertheless pay the price of neglecting potentially important effects as well as not addressing structural correlations with other vibrational bands. Consequently such simpler methods are expected to be less reliable, especially for simulations of VCD and Raman spectra, which depend on higher order optical properties that are best treated quantum mechanically. If one does utilize such simplified computational models for interactions and intensities, reliance on realistic structural models for peptides in sheets and fibrils appears to be critical for obtaining reliable results. Nevertheless, classical transition dipole coupling of DFT-modeled oscillators is a reasonable approximation for simulating the interactions between stacked sheets. Our combination of DFT and empirical TDC couplings thus allows accurate predictions of spectra of very large supramolecular structures.

ASSOCIATED CONTENT

Supporting Information

Summary of vibrational spectral simulations for model β-sheet structures. This material is available free of charge via the Internet at http://pubs.acs.org.

AUTHOR INFORMATION

Corresponding Author

*E-mail: tak@uic.edu (T.A.K.); jkubelka@uwyo.edu (J.K.).

Notes

The authors declare no competing financial interest.

ACKNOWLEDGMENTS

This work was supported in part by grants from the National Science Foundation (Grant CHE07-18543 to T.A.K. and CAREER 0846140 to J.K.) and by an Alexander von Humboldt Award (to T.A.K.). We thank Vaclav Profant, Charles University, Prague, for carrying out some early test calculations with various basis sets and functionals.

REFERENCES

(1) Barth, A.; Harris, P. I. Infrared Spectroscopy - Past and Present. In *Biological and Biomedical Infrared Spectroscopy*; Barth, A., Harris, P. I., Eds.; IOS Press: Amsterdam, The Netherlands, 2009; pp 1−52.

(2) Barth, A. Infrared Spectroscopy of Proteins. *Biochim. Biophys. Acta: Bioenerg.* **2007**, *1767*, 1073−1101.

(3) Keiderling, T. A.; Silva, R. A. G. D. Conformational Studies of Peptides with Infrared Techniques. In *Synthesis of Peptides and Peptidomimetics*; Goodman, M., Herrman, G., Eds.; Georg Thiem Verlag: Stuttgart, Germany, 2002; Vol. *22*, pp 715−738.

(4) Toniolo, C. F.; Formaggio, F.; Woody, R. W. Electronic Circular Dichroism of Peptides. In *Comprehensive Chiroptical Spectroscopy*; Berova, N., Polavarapu, P. L., Nakanishi, K., Woody, R. W., Eds.; John Wiley & Sons Inc.: Hoboken, NJ, 2012; Vol. *2*, pp 499−544.

(5) Salemme, F. R. Structural Properties of Protein Beta Sheets. *Prog. Biophys. Mol. Biol.* **1983**, *42*, 95−133.

(6) Eisenberg, D.; Jucker, M. The Amyloid State of Proteins in Human Diseases. *Cell* **2012**, *148*, 1188−1203.

(7) Nelson, R.; Eisenberg, D. Recent Atomic Models of Amyloid Fibril Structure. *Curr. Opin. Struct. Biol.* **2006**, *16*, 260−5.

(8) Tycko, R. Molecular Structure of Amyloid Fibrils: Insights from Solid-State NMR. *Q. Rev. Biophys.* **2006**, *39*, 1−55.

(9) Kubelka, J.; Keiderling, T. A. Differentiation of Beta-Sheet-Forming Structures: Ab Initio-Based Simulations of IR Absorption and Vibrational CD for Model Peptide and Protein Beta-Sheets. *J. Am. Chem. Soc.* **2001**, *123*, 12048−12058.

(10) Cerf, E.; Sarroukh, R.; Tamamizu-Kato, S.; Breydo, L.; Derclaye, S.; Dufrene, Y. F.; Narayanaswami, V.; Goormaghtigh, E.; Ruysschaert, J.-M.; Raussens, V. Anti-parallel Beta-Sheet: A Signature Structure of the Oligomeric Amyloid Beta-Peptide. *Biochem. J.* **2009**, *421*, 415−423.

(11) Choi, J. H.; Ham, S. Y.; Cho, M. Local Amide I Mode Frequencies and Coupling Constants in Polypeptides. *J. Phys. Chem. B* **2003**, *107*, 9132−9138.

(12) Lee, C.; Cho, M. Local Amide I Mode Frequencies and Coupling Constants in Multiple-Stranded Anti-Parallel β-Sheet Polypeptides. *J. Phys. Chem. B* **2004**, *108*, 20397−20407.

(13) Chirgadze, Y. N.; Nevskaya, N. A. Infrared Spectra and Resonance Interaction of Amide I Vibration of Anti-parallel Chain Pleated Sheet. *Biopolymers* **1976**, *15*, 607−625.

(14) Khurana, R.; Fink, A. L. Do Parallel β-Helix Proteins Have a Unique Fourier Transform Infrared Spectrum? *Biophys. J.* **2000**, *78*, 994−1000.

(15) Chirgadze, Y. N.; Nevskaya, N. A. Infrared Spectra and Resonance Interaction of Amide I Vibration of Parallel Chain Pleated Sheet. *Biopolymers* **1976**, *15*, 627−636.

(16) Karjalainen, E. L.; Ravi, H. K.; Barth, A. Simulation of the Amide I Absorption of Stacked β-Sheets. *J. Phys. Chem. B* **2011**, *115*, 749−757.

(17) Schweitzer-Stenner, R. Simulated IR, Isotropic and Anisotropic Raman, and Vibrational Circular Dichroism Amide I Band Profiles of Stacked β-Sheets. *J. Phys. Chem. B* **2012**, *116*, 4141−4153.

(18) Measey, T. J.; Schweitzer-Stenner, R. Vibrational Circular Dichroism as a Probe of Fibrillogenesis: The Origin of the Anomalous Intensity Enhancement of Amyloid-Like Fibrils. *J. Am. Chem. Soc.* **2011**, *133*, 1066−1076.

(19) Smith, A. W.; Tokmakoff, A. Probing Local Structural Events in β-Hairpin Unfolding with Transient Nonlinear Infrared Spectroscopy. *Angew. Chem., Int. Ed.* **2007**, *46*, 7984−7987.

(20) Woys, A. M.; Almeida, A. M.; Wang, L.; Chiu, C.-C.; McGovern, M.; de Pablo, J. J.; Skinner, J. L.; Gellman, S. H.; Zanni, M. T. Parallel Beta-Sheet Vibrational Couplings Revealed by 2D IR Spectroscopy of an Isotopically Labeled Macrocycle: Quantitative Benchmark for the Interpretation of Amyloid and Protein Infrared Spectra. *J. Am. Chem. Soc.* **2012**, *134*, 19118−19128.

(21) Moran, S. D.; Woys, A. M.; Buchanan, L. E.; Bixby, E.; Decatur, S. M.; Zanni, M. T. Two-Dimensional IR Spectroscopy and Segmental C-13 Labeling Reveals the Domain Structure of Human Gamma D-Crystallin Amyloid Fibrils. *Proc. Natl. Acad. Sci. U.S.A.* **2012**, *109*, 3329−3334.

(22) Wang, J.; Chen, J.; Hochstrasser, R. M. Local Structure of Beta-Hairpin Isotopomers by FTIR, 2D IR, and Ab Initio Theory. *J. Phys. Chem. B* **2006**, *110*, 7545−7555.

(23) Smith, A. W.; Lessing, J.; Ganim, Z.; Peng, C. S.; Tokmakoff, A.; Roy, S.; Jansen, T. L. C.; Knoester, J. Melting of a Beta-Hairpin Peptide Using Isotope-Edited 2D IR Spectroscopy and Simulations. *J. Phys. Chem. B* **2010**, *114*, 10913−10924.

(24) Decatur, S. M. Elucidation of Residue-Level Structure and Dynamics of Polypeptides via Isotope-Edited Infrared Spectroscopy. *Acc. Chem. Res.* **2006**, *39*, 169−175.

(25) Silva, R.; Kubelka, J.; Bouř, P.; Decatur, S. M.; Keiderling, T. A. Site-Specific Conformational Determination in Thermal Unfolding Studies of Helical Peptides Using Vibrational Circular Dichroism with Isotopic Substitution. *Proc. Natl. Acad. Sci. U.S.A.* **2000**, *97*, 8318−8323.

(26) Silva, R. A. G. D.; Barber-Armstrong, W.; Decatur, S. M. The Organization and Assembly of a Beta-Sheet Formed by a Prion Peptide in Solution: An Isotope-Edited FTIR Study. *J. Am. Chem. Soc.* **2003**, *125*, 13674−13675.

(27) Huang, R.; Kubelka, J.; Barber-Armstrong, W.; Silva, R.; Decatur, S. M.; Keiderling, T. A. Nature of Vibrational Coupling in Helical Peptides: An Isotopic Labeling Study. *J. Am. Chem. Soc.* **2004**, *126*, 2346−2354.

(28) Buchner, G. S.; Kubelka, J. Isotope-Edited Infrared Spectroscopy. In *Intrinsically Disordered Proteins Analysis: Vol. 1, Methods and Experimental Tools (Methods in Molecular Biology)*; Humana Press: Clifton, NJ, 2012; Vol. *1*, pp 347−358.

(29) Lansbury, P. T. J.; Costa, P. R.; Griffiths, J. M.; Simon, E. J.; Auger, M.; Halverson, K. J.; Kocisko, D. A.; Hendsch, Z. S.; Ashburn, T. T.; Spencer, R. G. Structural Model for the Beta-Amyloid Fibril Based on Interstrand Alignment of an Anti-parallel-Sheet Comprising a C-Terminal Peptide. *Nat. Struct. Biol.* **1995**, *2*, 990−998.

(30) Chimon, S.; Shaibat, M. A.; Jones, C. R.; Calero, D. C.; Aizezi, B.; Ishii, Y. Evidence of Fibril Like B-Sheet Structures in Neurotoxic Amyloid Intermediate of Alzheimers β-Amyloid. *Nat., Struct. Mol. Biol.* **2007**, *14*, 1157−1164.

(31) Petkova, A. T.; Ishii, Y.; Balbach, J. J.; Antzutkin, O. N.; Leapman, R. D.; Delaglio, F.; Tycko, R. A Structural Model for Alzheimer's Amyloid Fibrils Based on Experimental Constraints from Solid State NMR. *Proc. Natl. Acad. Sci. U.S.A.* **2002**, *99*, 16742−16747.

(32) Paul, C.; Wang, J. P.; Wimley, W. C.; Hochstrasser, R. M.; Axelsen, P. H. Vibrational Coupling, Isotopic Editing, and Beta-Sheet Structure in a Membrane-Bound Polypeptide. *J. Am. Chem. Soc.* **2004**, *126*, 5843−5850.

(33) Petty, S. A.; Decatur, S. M. Intersheet Rearrangement of Polypeptides During Nucleation of β-Sheet Aggregates. *Proc. Natl. Acad. Sci. U.S.A.* **2005**, *102*, 14272−14277.

(34) Mehta, A. K.; Lu, K.; Childers, W. S.; Liang, Y.; Dublin, S. N.; Dong, J.; Snyder, J. P.; Pingali, S. V.; Thiyagarajan, P.; Lynn, D. G. Facial Symmetry in Protein Self-Assembly. *J. Am. Chem. Soc.* **2008**, *130*, 9829−9835.

(35) Shanmugam, G.; Polavarapu, P. L. Isotope-Assisted Vibrational Circular Dichroism Investigations of Amyloid β Peptide Fragment, Aβ(16−22). *J. Struct. Biol.* **2011**, *176*, 212−219.

(36) Halverson, K.; Sucholeiki, I.; Ashburn, T. T.; Lansbury, P. T. Location of β-Sheet-Forming Sequences in Amyloid Proteins by FTIR. *J. Am. Chem. Soc.* **1991**, *113*, 6701−6703.

(37) Petty, S. A.; Decatur, S. M. Experimental Evidence for the Reorganization of Beta-Strands within Aggregates of the Abeta(16−22) Peptide. *J. Am. Chem. Soc.* **2005**, *127*, 13488−13489.

(38) Brauner, J. W.; Dugan, C.; Mendelson, R. ^{13}C Isotope Labeling of Hydrophobic Peptides. Origin of the Anomalous Intensity Distribution in the Infrared Amide I Spectral Region of Beta-Sheet. *J. Am. Chem. Soc.* **2000**, *122*, 677−683.

(39) Kubelka, J.; Keiderling, T. A. The Anomalous Infrared Amide I Intensity Distribution in C-13 Isotopically Labeled Peptide Beta-

Sheets Comes from Extended, Multiple-Stranded Structures. An Ab initio Study. *J. Am. Chem. Soc.* **2001**, *123*, 6142−6150.
(40) Huang, R.; Setnicka, V.; Etienne, M. A.; Kim, J.; Kubelka, J.; Hammer, R. P.; Keiderling, T. A. Cross-Strand Coupling of a β-Hairpin Peptide Stabilized with an Aib-Gly Turn Studied Using Isotope-Edited IR Spectroscopy. *J. Am. Chem. Soc.* **2007**, *129*, 13592−13603.
(41) Huang, R.; Wu, L.; McElheny, D.; Bouř, P.; Roy, A.; Keiderling, T. A. Cross-Strand Coupling and Site-Specific Unfolding Thermodynamics of a Trpzip β-Hairpin Peptide Using 13C Isotopic Labeling and IR Spectroscopy. *J. Phys. Chem. B* **2009**, *113*, 5661−5674.
(42) Hauser, K.; Krejtschi, C.; Huang, R.; Wu, L.; Keiderling, T. A. Site-Specific Relaxation Kinetics of a Tryptophan Zipper Hairpin Peptide Using Temperature-Jump IR Spectroscopy and Isotopic Labeling. *J. Am. Chem. Soc.* **2008**, *130*, 2984−2992.
(43) Hauser, K.; Ridderbusch, O.; Roy, A.; Krejtschi, C.; Hellerbach, A.; Huang, R.; Keiderling, T. A. Isotopic Substitution Methods for Equilibrium and T-Jump Studies of Peptide Conformation. *J. Phys. Chem. B* **2010**, *114*, 11628−11637.
(44) Hilario, J.; Kubelka, J.; Keiderling, T. A. Optical Spectroscopic Investigations of Model Beta-Sheet Hairpins in Aqueous Solution. *J. Am. Chem. Soc.* **2003**, *125*, 7562−7574.
(45) Wu, L.; McElheny, D.; Huang, R.; Keiderling, T. A. Role of Tryptophan-Tryptophan Interactions in Trpzip β-Hairpin Formation, Structure, and Stability. *Biochemistry* **2009**, *48*, 10362−10371.
(46) Wu, L.; McElheny, D.; Takekiyo, T.; Keiderling, T. A. Geometry and Efficacy of Cross-Strand Trp/Trp, Trp/Tyr, and Tyr/Tyr Aromatic Interaction in a β-Hairpin Peptide. *Biochemistry* **2010**, *49*, 4705−4714.
(47) Wu, L.; McElheny, D.; Setnička, V.; Hilario, J.; Keiderling, T. A. Role of Different β-Turns in β-Hairpin Conformation and Stability Studied by Optical Spectroscopy. *Proteins* **2012**, *80*, 44−60.
(48) Torii, H.; Taumi, M. Ab Initio Molecular Orbital Study of the Amide I Vibrational Interactions between the Peptide Groups in Di- and Tripeptides and Considerations on the Conformation of the Extended Helix. *J. Raman Spectrosc.* **1998**, *29*, 81−86.
(49) Kubelka, J.; Bouř, P.; Keiderling, T. A. Quantum Mechanical Calculations of Peptide Vibrational Force Fields and Spectral Intensities. In *Biological and Biomedical Infrared Spectroscopy*; Barth, A., Haris, P. I., Eds.; IOS Press: Amsterdam, The Netherlands, 2009; Vol. 2, pp 178−223.
(50) Bouř, P.; Sopková, J.; Bednárová, L.; Maloň, P.; Keiderling, T. A. Transfer of Molecular Property Tensors in Cartesian Coordinates: A New Algorithm for Simulation of Vibrational Spectra. *J. Comput. Chem.* **1997**, *18*, 646−659.
(51) Gorbunov, R. D.; Nguyen, P. H.; Kobus, M.; Stock, G. Quantum-Classical Description of the Amide I Vibrational Spectrum of Trialanine. *J. Chem. Phys.* **2007**, *126*, 054509.
(52) Kubelka, J. Vibrational Spectroscopic Studies of Peptide and Protein Structures. Theory and Experiment. Ph.D Thesis, University of Illinois at Chicago, Chicago, IL, 2002.
(53) Bouř, P.; Keiderling, T. A. Structure, Spectra and the Effects of Twisting of Beta-Sheet Peptides. A Density Functional Theory Study. *J. Mol. Struct. (Theochem)* **2004**, *675*, 95−105.
(54) Bouř, P.; Keiderling, T. A. Ab Initio Modeling of Amide I Coupling in Anti-Parallel β-Sheets and the Effect of the ^{13}C Isotopic Labeling on Vibrational Spectra. *J. Phys. Chem. B* **2005**, *109*, 5348−5357.
(55) Kubelka, J.; Kim, J.-H.; Bouř, P.; Keiderling, T. A. Contribution of Transition Dipole Coupling to Amide Coupling in IR Spectra of Peptide Secondary Structures. *Vib. Spectrosc.* **2006**, *42*, 63−73.
(56) Bouř, P.; Keiderling, T. A. Empirical Modeling of the Peptide Amide I Band IR Intensity in Water Solution. *J. Chem. Phys.* **2003**, *119*, 11253−11262.
(57) Bouř, P.; Michalík, D.; Kapitán, J. Empirical Solvent Correction for Multiple Amide Group Vibrational Modes. *J. Chem. Phys.* **2005**, *122*, 144501.
(58) Kubelka, J.; Huang, R.; Keiderling, T. A. Solvent Effects on IR and VCD Spectra of Helical Peptides: DFT-Based Static Spectral Simulations with Explicit Water. *J. Phys. Chem. B* **2005**, *109*, 8231−8243.
(59) Turner, D. R.; Kubelka, J. Infrared and Vibrational CD Spectra of Partially Solvated Alpha-Helices: DFT-Based Simulations with Explicit Solvent. *J. Phys. Chem. B* **2007**, *111*, 1834−1845.
(60) Grahnen, J. A.; Amunson, K. E.; Kubelka, J. DFT-Based Simulations of IR Amide I′ Spectra for a Small Protein in Solution. Comparison of Explicit and Empirical Solvent Models. *J. Phys. Chem. B* **2010**, *114*, 13011−13020.
(61) Welch, W. R. W.; Kubelka, J. DFT-Based Simulations of Amide I′ IR Spectra of a Small Protein in Solution Using Empirical Electrostatic Map with a Continuum Solvent Model. *J. Phys. Chem. B* **2012**, *116*, 10739−10747.
(62) Welch, W. R. W.; Keiderling, T. A.: Kubelka, J. Structural Analyses of Experimental ^{13}C Edited Amide I′ IR and VCD for Peptide β-Sheet Aggregates and Fibrils Using DFT-Based Spectral Simulations. *J. Phys. Chem. B* **2013**, DOI: 10.1021/jp405613r.
(63) Bouř, P.; Kubelka, J.; Keiderling, T. A. Simulations of Oligopeptide Vibrational Circular Dichroism. Effects of Isotopic Labeling. *Biopolymers* **2000**, *53*, 380−395.
(64) Kubelka, J.; Silva, R. A. G. D.; Bouř, P.; Decatur, S. M.; Keiderling, T. A. Chirality in Peptide Vibrations. Ab Initio Computational Studies of Length, Solvation, Hydrogen Bond, Dipole Coupling and Isotope Effects on Vibrational CD. In *Chirality: Physical Chemistry*; ACS Symposium Series, Vol. *810*; Hicks, J. M., Ed.; American Chemical Society: Washington, DC, 2002; pp 50−64.
(65) Frisch, M. J.; Trucks, G. W.; Schlegel, H. B.; Scuseria, G. E.; Robb, M. A.; Cheeseman, J. R.; Scalmani, G.; Barone, V.; Mennucci, B.; Petersson, G. A.; Nakatsuji, H.; Caricato, M.; Li, X.; Hratchian, H. P.; Izmaylov, A. F.; Bloino, J.; Zheng, G.; Sonnenberg, J. L.; Hada, M.; Ehara, M.; Toyota, K.; Fukuda, R.; Hasegawa, J.; Ishida, M.; Nakajima, T.; Honda, Y.; Kitao, O.; Nakai, H.; Vreven, T.; Montgomery, J. A., Jr.; Peralta, J. E.; Ogliaro, F.; Bearpark, M.; Heyd, J. J.; Brothers, E.; Kudin, K. N.; Staroverov, V. N.; Kobayashi, R.; Normand, J.; Raghavachari, K.; Rendell, A.; Burant, J. C.; Iyengar, S. S.; Tomasi, J.; Cossi, M.; Rega, N.; Millam, J. M.; Klene, M.; Knox, J. E.; Cross, J. B.; Bakken, V.; Adamo, C.; Jaramillo, J.; Gomperts, R.; Stratmann, R. E.; Yazyev, O.; Austin, A. J.; Cammi, R.; Pomelli, C.; Ochterski, J. W.; Martin, R. L.; Morokuma, K.; Zakrzewski, V. G.; Voth, G. A.; Salvador, P.; Dannenberg, J. J.; Dapprich, S.; Daniels, A. D.; Farkas, O.; Foresman, J. B.; Ortiz, J. V.; Cioslowski, J.; Fox, D. J. *Gaussian 09*; Gaussian, Inc.: Wallingford, CT, 2009.
(66) Kubelka, J.; Bouř, P. Simulation of Vibrational Spectra of Large Molecules by Arbitrary Time Propagation. *J. Chem. Theory Comput.* **2009**, *5*, 200−207.
(67) Cai, S. W.; Singh, B. R. A Distinct Utility of the Amide III Infrared Band for Secondary Structure Estimation of Aqueous Protein Solutions Using Partial Least Squares Methods. *Biochemistry* **2004**, *43*, 2541−2549.
(68) Asher, S. A.; Ianoul, A.; Mix, G.; Boyden, M. N.; Karnoup, A.; Diem, M.; Schweitzer-Stenner, R. Dihedral Psi Angle Dependence of the Amide III Vibration: A Uniquely Sensitive UV Resonance Raman Secondary Structural Probe. *J. Am. Chem. Soc.* **2001**, *123*, 11775−11781.
(69) Huang, C. Y.; Balakrishnan, G.; Spiro, T. G. Protein Secondary Structure from Deep-UV Resonance Raman Spectroscopy. *J. Raman Spectrosc.* **2006**, *37*, 277−282.
(70) Kurouski, D.; Lombardi, R. A.; Dukor, R. K.; Lednev, I. K.; Nafie, L. A. Direct Observation and pH Control of Reversed Supramolecular Chirality in Insulin Fibrils by Vibrational Circular Dichroism. *Chem. Commun.* **2010**, *46*, 7154−7156.
(71) Kurouski, D.; Dukor, R. K.; Lu, X.; Nafie, L. A.; Lednev, I. K. Normal and Reversed Supramolecular Chirality of Insulin Fibrils Probed by Vibrational Circular Dichroism at the Protofilament Level of Fibril Structure. *Biophys. J.* **2012**, *103*, 522−531.
(72) Fulara, A.; Lakhani, A.; Wojcik, S.; Nieznanska, H.; Keiderling, T. A.; Dzwolak, W. Spiral Superstructures of Amyloid-Like Fibrils of Polyglutamic Acid: An Infrared Absorption and Vibrational Circular Dichroism Study. *J. Phys. Chem. B* **2011**, *115*, 11010−11016.

(73) Surmacz-Chwedoruk, W.; Nieznanska, H.; Wojcik, S.; Dzwolak, W. Cross-Seeding of Fibrils from Two Types of Insulin Induces New Amyloid Strains. *Biochemistry* **2012**, *51*, 9460−9469.
(74) Chi, H.; Welch, W. R. W.; Kubelka, J.; Keiderling, T. A. Insight into the Packing Pattern of Beta-2 Fibrils: A Model Study of Glutamic Acid Rich Oligomers with ^{13}C Isotopically Edited Vibrational Spectroscopy. Submitted for publication.
(75) Torii, H.; Tasumi, M. Model Calculations on the Amide-I Infrared Bands of Globular Proteins. *J. Chem. Phys.* **1992**, *96*, 3379−3387.
(76) Viswanathan, R.; Dannenberg, J. J. A Density Functional Theory Study of Vibrational Coupling in the Amide I Band of Beta-Sheet Models. *J. Phys. Chem. B* **2008**, *112*, 5199−5208.
(77) Polzi, L. Z.; Daidone, I.; Amadei, A.; Theoretical, A. Reappraisal of Polylysine in the Investigation of Secondary Structure Sensitivity of Infrared Spectra. *J. Phys. Chem. B* **2012**, *116*, 3353−3360.
(78) Lee, H.; Kim, S. S.; Choi, J. H.; Cho, M. Theoretical Study of Internal Field Effects on Peptide Amide I Modes. *J. Phys. Chem. B* **2005**, *109*, 5331−5340.
(79) Bouř, P.; Keiderling, T. A. Ab-Initio Simulations of the Vibrational Circular Dichroism of Coupled Peptides. *J. Am. Chem. Soc.* **1993**, *115*, 9602−9607.
(80) Tycko, R.; Wickner, R. B. Molecular Structures of Amyloid and Prion Fibrils: Consensus Versus Controversy. *Acc. Chem. Res.* **2013**, *46*, 1487−1496.